A Fluid Model for the Interaction of the Solar Wind and the Geomagnetic Field

John R. Spreiter, Audrey L. Summers, and Alberta Y. Alksne

Ames Research Center, NASA,

Moffett Field, California

Data obtained in space, particularly that from IMP-1, have established that many of the gross features of the interaction of the solar wind and the geomagnetic field can be described by the continuum theory of fluid flow. The purpose of this paper is twofold: (a) to indicate briefly how one can arrive at results for the magnetosphere boundary, the bow wave, and the associated flow field from a purely fluid point of view without resort to a mixture of particle and fluid models as usually employed and (b) to present numerical results for the flow parameters in the shock layer between the bow wave and the magnetosphere boundary. The objective is not to get a complicated theory that encompasses all phenomena of importance, but rather the simplest body of analysis that appears able to describe the average bulk properties of the solar wind as it flows steadily through the bow wave and around the forward portion of the magnetosphere. A more complete account of this study is given by Spreiter et. al. (1965).

The fundamental assumption is that the flow can be described adequately by the standard magnetohydrodynamic equations for steady flow of a dissipationless perfect gas. No attempt will be made here to justify this assumption in detail, except to remark that the presence of a weak and irregular magnetic field in the incident solar wind plasma seems

sufficient to couple the motions of the particles even in the absence of collisions. The differential equations are thus as follows (see, e.g., Landau and Lifshitz, 1960).

$$\left.\begin{aligned} &\nabla \cdot \rho \underset{\sim}{v} = 0 \\ &\rho(\underset{\sim}{v} \cdot \underset{\sim}{\nabla})\underset{\sim}{v} + \nabla p = -\frac{1}{4\pi}\underset{\sim}{H} \times \underset{\approx}{\mathrm{curl}}\,\underset{\sim}{H} = -\frac{1}{8\pi}\nabla H^2 + \frac{1}{4\pi}(\underset{\sim}{H} \cdot \underset{\sim}{\nabla})\underset{\sim}{H} \\ &\underset{\approx}{\mathrm{curl}}(\underset{\sim}{H} \times \underset{\sim}{v}) = 0 , \qquad \mathrm{div}\,\underset{\sim}{H} = 0 \\ &(\underset{\sim}{v} \cdot \underset{\sim}{\nabla})S = 0 , \qquad p = e^{S/c_v}\rho^{\gamma} \end{aligned}\right\} \quad (1)$$

where ρ, p, S, and $\underset{\sim}{v}$ refer to the density, pressure, entropy, and velocity of the gas, $\underset{\sim}{H}$ refers to the magnetic field, $\gamma = c_p/c_v$, and c_p and c_v are constants representing the specific heats at constant pressure and constant volume. Important auxiliary relations for γ, temperature T, speed of sound a, internal energy e, and enthalpy h are

$$\left.\begin{aligned} &\gamma = (N + 2)/N , \qquad p = \rho RT/\mu = nkT \\ &a = (\partial p/\partial \rho)^{1/2} = (\gamma p/\rho)^{1/2} = (\gamma RT/\mu)^{1/2} \\ &e = c_v T, \; h = c_p T = e + p/\rho \end{aligned}\right\} \quad (2)$$

where N represents the number of degrees of freedom, $R = (c_p - c_v)\mu = 8.314\times10^7$ erg/$^\circ$K, μ = mean molecular weight = 1/2 for fully ionized hydrogen plasma, n = number of particles/cm^3 = $2n_p$ where n_p is the number of protons/cm^3, and k = Boltzmann's constant = 1.38×10^{-16} erg/$^\circ$K.

[redacted]

Although only first derivatives appear in this system of equations, the neglected dissipative terms are described by second derivatives. Their neglect requires that the gradients be small. In magnetohydrodynamics, as in gasdynamics, however, compressions tend to coalesce and steepen into shock waves of such small thickness that they can be considered as virtual discontinuities. In addition, attraction between like currents tends to cause current distributions to collapse into thin sheaths, across which the magnetic field can be considered in the same sense to be nearly discontinuous. Mathematically, continuous solutions of the dissipationless differential equations cease to exist, and the flow is no longer governed solely by the equations given above. Mass, momentum, magnetic flux, and energy must still be conserved, however, and the following relations must hold between quantities on the two sides of any such discontinuity:

$$\left.\begin{aligned} [\rho v_n] &= 0 \\ \left[\rho v_n \underset{\approx}{v} + \left(p + \frac{H^2}{8\pi}\right)\hat{n} - \frac{1}{4\pi} H_n \underset{\approx}{H}_t\right] &= 0 \\ \left[\rho v_n \underset{\approx}{v}_t - \frac{1}{4\pi} H_n \underset{\approx}{H}_t\right] &= 0 , \qquad [H_n] = 0 \\ \left[\rho v_n \left(\frac{1}{2} v_n^2 + h\right) + v_n \frac{H^2}{4\pi} - \frac{1}{4\pi} H_n \underset{\approx}{v} \cdot \underset{\approx}{H}\right] &= 0 \end{aligned}\right\} \quad (3)$$

The subscripts n and t refer to components normal and tangential to the discontinuity surface and $[Q] = Q_1 - Q_0$ where subscripts 0 and 1 refer to conditions on the upstream and downstream sides of the discontinuity.

Five classes of discontinuities are described by equation (3). Following Landau and Lifshitz (1960), discontinuities which lie along streamlines ($v_n = 0$) are called tangential discontinuities or contact discontinuities according to whether or not the normal component of the magnetic field H_n vanishes. Discontinuities across which there is flow ($v_n \neq 0$) are divided into three categories called rotational discontinuities, and fast and slow shock waves. Some properties that distinguish the various discontinuities are summarized below:

Tangential discontinuities

$$v_n = H_n = 0 \; ; \quad [\underset{\approx}{v}_t] \neq 0 \; , \quad [\underset{\approx}{H}_t] \neq 0 \; , \quad [\rho] \neq 0 \; , \quad [p + H^2/8\pi] = 0 \tag{4}$$

Contact discontinuities

$$v_n = 0 \; , \quad H_n \neq 0 \; : \quad [\underset{\approx}{v}] = [\underset{\approx}{H}] = [p] = 0 \; , \quad [\rho] \neq 0 \tag{5}$$

Rotational discontinuities

$$\left.\begin{aligned} &v_n = \pm H_n/(4\pi\rho)^{1/2} \; , \quad [\underset{\approx}{v}_t] = [\underset{\approx}{H}_t]/(4\pi\rho)^{1/2}, \\ &[\rho] = [p] = [v_n] = [H_n] = [H^2] = 0 \end{aligned}\right\} \tag{6}$$

Shock waves, fast and slow

$$\left.\begin{aligned} &v_n \neq 0 \; , \; [\rho] > 0 \; , \quad [H_n] = 0 \; , \\ &(\rho v_n)_{\text{fast}} \geq (\rho v_n)_{\text{rot}} = H_n(\rho/4\pi)^{1/2} \geq (\rho v_n)_{\text{slow}} \\ &\underset{\approx}{H}_t \quad \text{and} \quad H^2 \begin{pmatrix} \text{increase} \\ \text{decrease} \end{pmatrix} \quad \text{through} \quad \begin{pmatrix} \text{fast} \\ \text{slow} \end{pmatrix} \quad \text{shock waves} \end{aligned}\right\} \tag{7}$$

Of these, only the tangential discontinuity has properties compatible with those required to describe the boundary of the geomagnetic field. As in the classical Chapman-Ferraro theory based on particle concepts, the condition $H_n = 0$ holds and requires that there is no connectivity between the geomagnetic and interplanetary fields. Slight differences stem from the additional assumptions in the Chapman-Ferraro theory that the incident plasma is free of magnetic field and the outer magnetosphere is free of plasma so that $p_o = H_1^2/8\pi$. Although neither of these statements is strictly true, estimates of the magnitudes of the gas pressure p and the magnetic pressure $H^2/8\pi$ lead to the conclusion that $p \ll H^2/8\pi$ in the outer magnetosphere and that $p \gg H^2/8\pi$ in the shock layer. So far as the flow outside the magnetosphere is concerned, the discontinuities at the magnetosphere boundary may thus be approximated satisfactorily by those of the limiting case of a tangential discontinuity in which there is a vacuum on one side, and negligible magnetic pressure on the other side. It is demonstrated further by Spreiter et. al. (1965) that the gas pressure on the magnetosphere boundary is adequately approximated by the simple Newtonian formula $p = K\rho_\infty v_\infty^2 \cos^2\psi$ where the subscript ∞ refers to the values in the undisturbed incident stream, ψ is the angle between the normal to the boundary and the velocity vector of the undisturbed stream, and K is a constant usually taken to be unity but which yields better accuracy if equated to 0.84 for $\gamma = 2$ and 0.88 for $\gamma = 5/3$. In this way, the calculation of the shape of the magnetosphere boundary is decoupled from the detailed analysis of the surrounding flow and reduced to the identical mathematical problem described by the classical Chapman-Ferraro theory.

Examination of conditions typical of the solar wind shows that the mass flux ρv_n through the nose of the bow wave is characteristically about an order of magnitude greater than that through a rotational discontinuity. The bow wave must therefore be a fast shock wave.

Although it has been necessary to invoke the presence of a magnetic field to provide a mechanism for providing interactions between the particles, and to consider the complications of hydromagnetic theory to provide an adequate description of the magnetosphere boundary as a tangential discontinuity and the bow wave as a fast hydromagnetic shock wave, the magnetic field strengths typically encountered in the solar wind are sufficiently small as otherwise to produce only secondary effects on the flow. On this basis, one can justify the neglect of all the terms containing the magnetic field $\underset{\approx}{H}$ in equations (1) and (3) when calculating the flow. The fluid motion then calculated is just exactly that indicated by ordinary gasdynamic theory. Deformations of the magnetic field are determined subsequently using the equations

$$\operatorname{curl} (\underset{\approx}{H} \times \underset{\approx}{v}) = 0 , \quad \operatorname{div} \underset{\approx}{H} = 0 , \quad [H_n] = 0 \tag{8}$$

which are frequently interpreted as indicating the magnetic field lines move with the fluid.

In this way, the exterior magnetosphere flow problem is reduced to a purely gasdynamic problem of supersonic flow past a given body, the shape of which is determined by solving the standard Chapman-Ferraro problem. Difficulties associated with the nonlinear and mixed elliptic-hyperbolic character of the governing partial differential equations are such, however, that it is necessary at the present time to approximate

the magnetosphere boundary with an axisymmetric shape. The precise shape selected is that obtained by rotating the equatorial trace of the boundary given by the approximate solution of Spreiter and Briggs (1962) about an axis through the center of the earth that extends parallel to the velocity vector of the undisturbed incident stream.

The principal gasdynamic result presented by Spreiter and Jones (1963) was a plot of the calculated position of the bow shock wave associated with the simplified axisymmetric magnetosphere described in the preceding paragraph. The calculations were performed for a ratio of specific heats γ of 2, and a free-stream Mach number of 8.71. The latter was identified with the free-stream Alfvén Mach number associated with a representative choice of values for the density, velocity, and magnetic field of the incident solar wind. It is implicit in the analysis presented above, however, that the gasdynamic Mach number should more properly be identified with the free-stream Mach number $M_\infty = v_\infty/a_\infty$ than the Alfvén Mach number $M_{A_\infty} = v_\infty(4\pi\rho/H^2)^{1/2}$ if M_{A_∞} is much greater than unity, as is indeed generally the case in the present applications. Since a value of 8.71 is also a reasonable choice for M_∞, we turn now to a presentation of further details of the flow field for the same set of conditions as employed by Spreiter and Jones (1963).

Figure 1 shows a plot of the magnetosphere boundary and shock wave position for $\gamma = 2$ and $M_\infty = 8.71$ in terms of a length scale in which the distance D from the center of the earth to the magnetosphere nose is unity. D is generally of the order of 10 earth radii, and fluctuates in response to variations in the incident stream in accordance with the expression $D = a_e H p_o^{1/3}/(2\pi K \rho_\infty v_\infty^2)^{1/6}$ where $a_e = 6.37\times10^8$ cm is the

radius of the earth and $H_{p_o} = 0.312$ gauss is the intensity of the earth's magnetic field at the equator. Also included on this figure are several solid lines representing streamlines, and broken lines representing characteristic or Mach lines of the flow. The latter correspond to standing compression or expansion waves of infinitesimal amplitude. They cross the streamlines at such angles that the local velocity component normal to the wave is exactly equal to the local sound speed. Mach lines thus exist only where the flow is supersonic; they are absent from the vicinity of the magnetosphere nose because the flow there is subsonic.

Contour maps showing lines of constant density, velocity, temperature, and mass flux, each normalized by dividing by the corresponding quantity in the incident stream are presented in Figure 2. The results show that the density ratio ρ/ρ_∞ remains close to the maximum value $(\gamma + 1)/(\gamma - 1) = 3$ for a strong shock wave in a gas with $\gamma = 2$ along nearly the entire length of the portion of the bow wave shown. The gas undergoes a small additional compression as it approaches the stagnation point at the magnetosphere nose and then expands to less than free-stream density as it flows around the magnetosphere. The velocity remains less than in the free stream, however, throughout the same region. The temperature T/T_∞ is closely related to the velocity ratio through the expression

$$\frac{T}{T_\infty} = 1 + \frac{(\gamma - 1)M_\infty^2}{\gamma}\left(1 - \frac{v^2}{v_\infty^2}\right) \qquad (9)$$

derived from equations (1) and (2) with $\underset{\sim}{H} = 0$. Of particular interest is the tremendous increase in temperature of the solar wind as it passes

through the bow shock wave. If, for example, the temperature of the incident solar wind is $50{,}000^{\circ}$ K, the temperature at the magnetosphere nose is indicated to be nearly $2{,}000{,}000^{\circ}$ K. This value is consistent with the temperature possessed by the gas in the solar corona before it is accelerated to the high velocities characteristic of the solar wind in the vicinity of the earth's orbit.

As noted above, calculation of the deformation of the magnetic field in the flow around the magnetosphere can be accomplished directly, once the flow field is determined, either by direct integration of equation (8) or by considering the field lines to move with the fluid. Although the field lines are, in general, spatial curves, simplicity may be achieved at the expense of completeness by confining attention to the plane containing the velocity and magnetic field vectors in the incident stream. Since the magnetosphere has been approximated by an axisymmetric shape, it follows that the resulting field lines for this case are also confined entirely to the same plane. Results of two such calculations are shown in Figure 3. The magnetic field in the incident stream is inclined at 90° to the direction of the velocity vector in the left portion of Figure 3, and 45° in the right portion. The corresponding results for 0° inclination are not presented, but can be visualized easily because the field lines for that case are aligned everywhere with the streamlines, and the field strength ratio H/H_{∞} is proportional to $\rho v/\rho_{\infty} v_{\infty}$.

These results clearly show how the magnetic field lines bend discontinuously as they pass through the bow wave at any angle except a right angle, and then curve in a continuous manner throughout the entire

region between the bow wave and the magnetosphere. The discontinuous bend at the shock wave is, moreover, always in the direction that preserves the sign of the tangential component of the field, as is required for all physically relevant hydromagnetic shock waves. It may be seen that the field lines illustrated in Figure 3 are all draped around the nose of the magnetosphere. Outside of this plane, however, the field lines drift past the nose with the flow and deform into three-dimensional curves. The strong constraint imposed on the magnetic field by the stagnation point is thus greatly reduced, and the field lines may be anticipated to remain much straighter than illustrated for the plane of symmetry.

The choice of the value 2 for the ratio of specific heats employed in calculating Figures 2 and 3 is usually justified by reference to the presumed two-degree-of-freedom nature of the interactions of charged particles in a magnetic field. This argument weakens, however, when consideration is given to the irregular character of the magnetic fields observed in space, particularly downstream of the bow shock wave. In fact, the whole concept of applying hydromagnetic theory to the flow of solar plasma around the magnetosphere involving as it does the assumption of an isotropic pressure appears more consistent internally if the particles are considered to behave as if they have three rather than two degrees of freedom and γ is equated to 5/3. The effects on the velocity and temperature contours of changing γ from 2 to 5/3 are shown in Figure 4.

Although the values of 8 and 8.71 employed in Figures 2, 3, and 4 for the free-stream Mach number are well centered in the range of values

to be expected in the incident solar wind, considerable variation is known to occur. In order to illustrate the magnitude of the effects to be anticipated, results are presented in Figure 5 for Mach numbers of 5 and 12 for a gas with $\gamma = 5/3$. They show that the bow wave recedes from the magnetosphere as the Mach number diminishes and as γ increases. The change is small in the ranges covered, however, as is the change in the velocity contours. Temperatures in the flow field depend strongly on both Mach number and γ, however, with higher values associated with higher Mach number and larger γ.

A useful quantity for characterizing the location of the bow shock wave is the standoff distance Δ at the nose of the magnetosphere. This distance has been shown in an aerodynamic context by Seiff (1962) and Inouye (1965) to be very nearly proportional to the density ratio across the nose of the bow wave for a wide range of values for γ and M_∞. The degree to which this simple empirical result is able to represent the standoff distance is illustrated in Figure 6.

In conclusion, we have presented a sample of the type of results that can be obtained using the continuum equations of magnetohydrodynamics and gasdynamics. They augment the results for the location of the bow wave given by Spreiter and Jones (1963) which has been widely used in the interpretation of data from IMP-1 satellite and Mariner 2 and 4 space probes. It has been reported in this symposium by Coon that data from the Vela satellites are in at least qualitative agreement with these results. With respect to such comparisons, it should be observed that our calculations only yield information regarding the average bulk properties of the flow, whereas the usual plasma probes and magnetometers

observe a much more microscopic and instantaneous view of the plasma. With respect to the latter, it should also be recalled that substantial quantitative discrepancies still remain between the values for bulk parameters deduced from readings of plasma probes of different design even when flown on the same spacecraft. These differences are certain to be resolved as better understanding develops, and we present these results at this time in order that they be available for comparison with observational data as the latter becomes increasingly available.

REFERENCES

Inouye, M.: 1965, AIAA J. 3, 172.

Landau, L. D., and Lifshitz, E. M.: 1960, Electrodynamics of Continuous Media, Pergamon Press, Oxford-New York.

Seiff, A.: 1962, Gasdynamics in Space Exploration, NASA SP-24.

Spreiter, J. R., and Briggs, B. R.: 1962, J. Geophys. Res. 67, 37.

Spreiter, J. R., and Jones, W. P.: 1963, J. Geophys. Res. 68, 3555.

Spreiter, J. R., Summers, A. L., and Alksne, A. Y.: 1965, Plan. Space Sci. (in press).

FIGURE CAPTIONS

Figure 1.- Streamlines and wave patterns for supersonic flow past the magnetosphere; $M_\infty = 8.71$, $\gamma = 2$.

Figure 2.- Contour maps of constant velocity, mass flux, density, and temperature for supersonic flow past the magnetosphere; $M_\infty = 8.71$, $\gamma = 2$.

Figure 3.- Magnetic field lines in plane of free-stream velocity and magnetic field vectors for supersonic flow past the magnetosphere; $M_\infty = 8.71$, $\gamma = 2$.

Figure 4.- Effect on velocity and temperature contours of changing ratio of specific heats from 2 to 5/3; $M_\infty = 8$.

Figure 5.- Effect on velocity and temperature contours of changing Mach number to 5 and 12; $\gamma = 5/3$.

Figure 6.- Variation of standoff distance with density ratio across the nose of the bow shock wave.

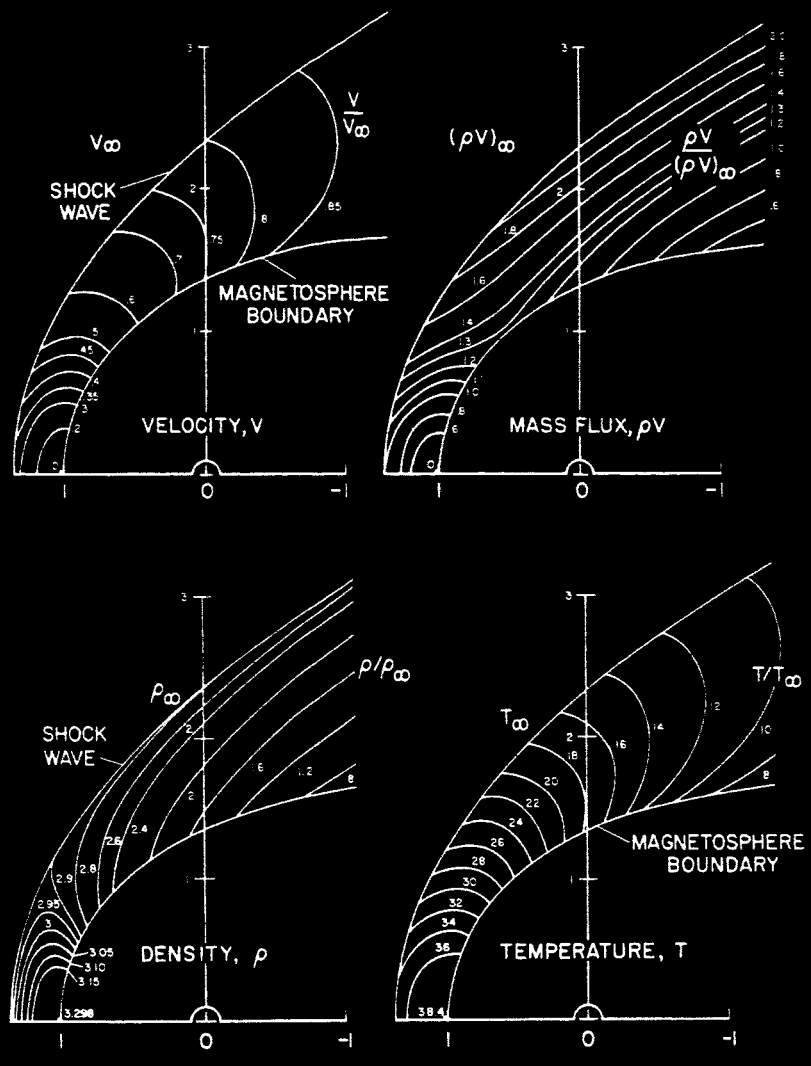

Fig. 2. Contour maps of constant velocity, mass flux, density, and temperature for supersonic flow past the magnetosphere; $M_\infty = 8.71$, $\gamma = 2$.

NATIONAL AERONAUTICS AND SPACE ADMINISTRATION
AMES RESEARCH CENTER, MOFFETT FIELD, CALIFORNIA

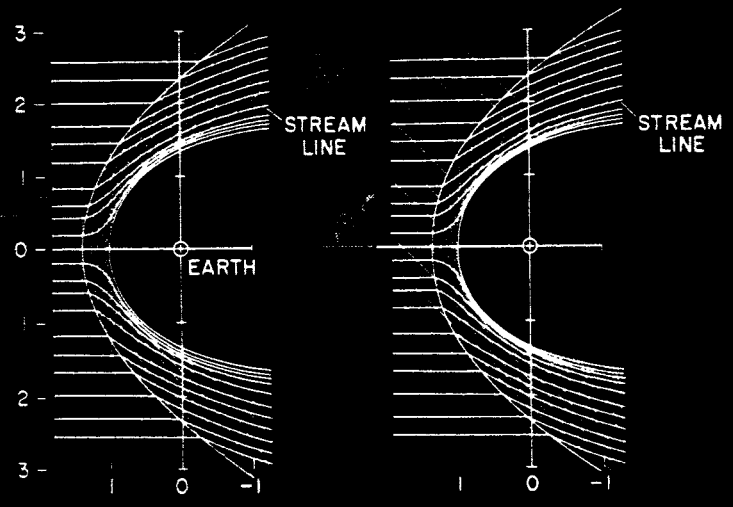

Fig. 3. Magnetic field lines in plane of free-stream velocity and magnetic field vectors for supersonic flow past the magnetosphere; M_∞ = 3., γ = 2.

NATIONAL AERONAUTICS AND SPACE ADMINISTRATION
AMES RESEARCH CENTER, MOFFETT FIELD, CALIFORNIA

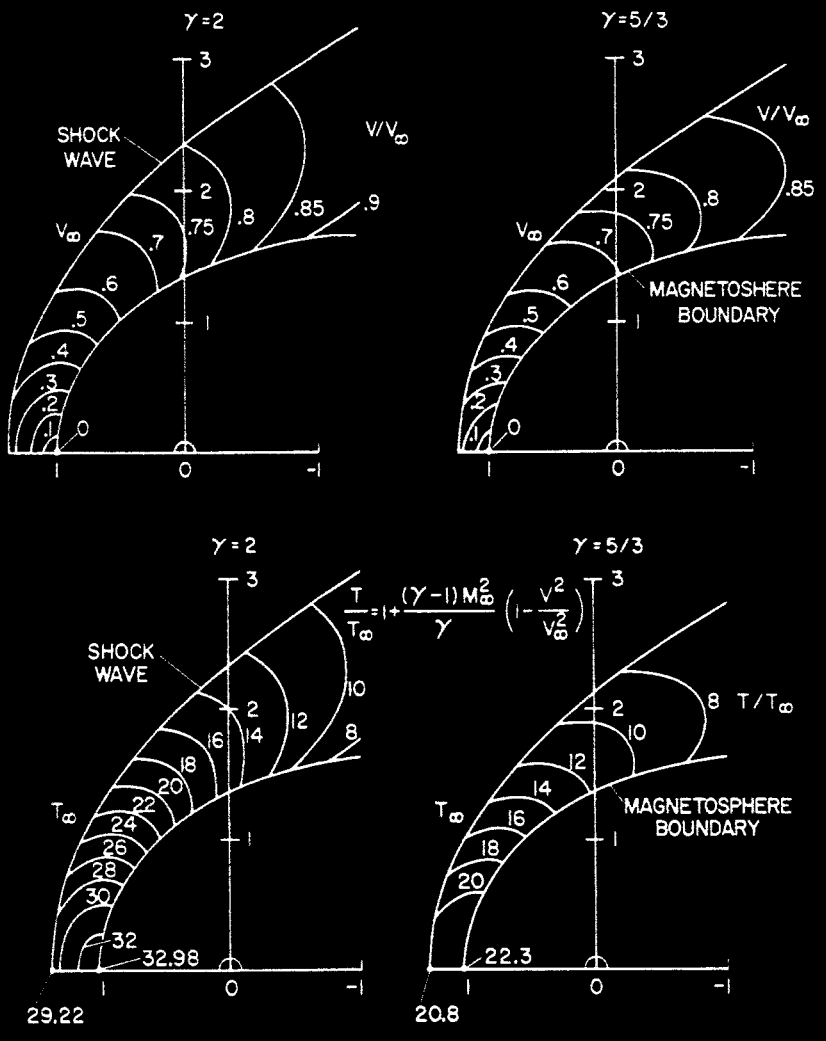

Fig. 4. Effect on velocity and temperature contours of changing ratio of specific heats from 2 to 5/3; $M_\infty = 8$.

NATIONAL AERONAUTICS AND SPACE ADMINISTRATION
AMES RESEARCH CENTER, MOFFETT FIELD, CALIFORNIA

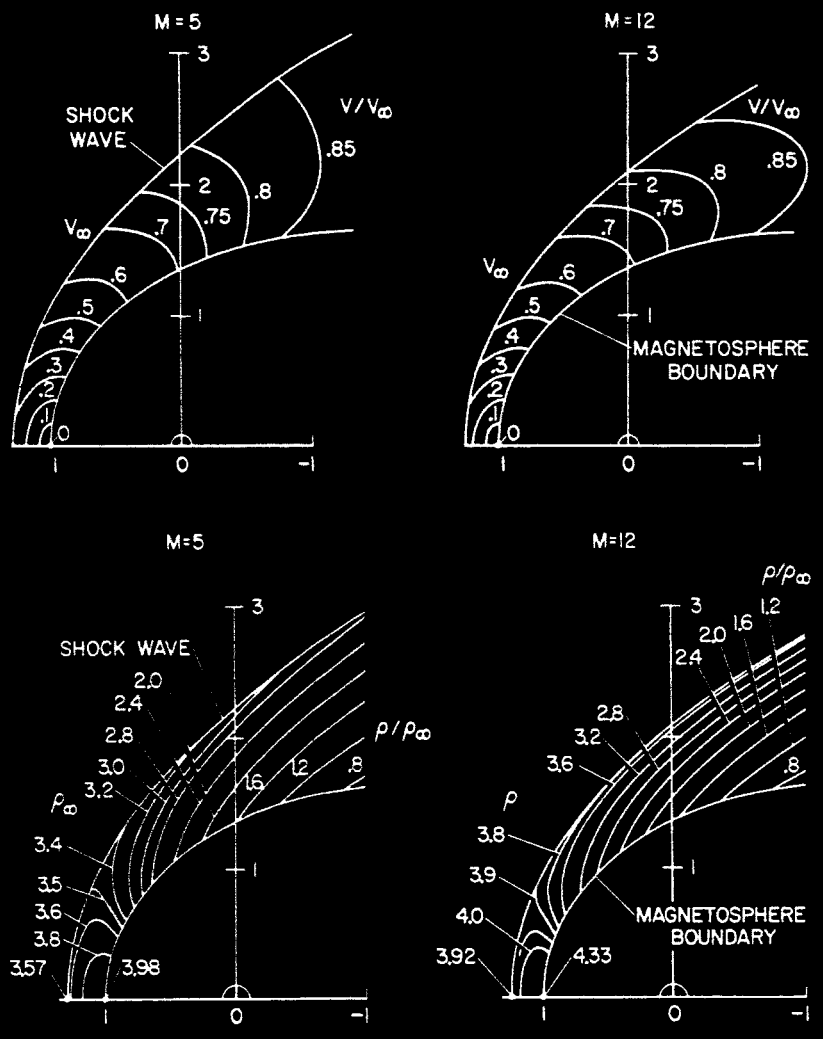

Fig. 5. Effect on velocity and temperature contours of changing Mach number to 5 and 12; $\gamma = 5/3$.

NATIONAL AERONAUTICS AND SPACE ADMINISTRATION
AMES RESEARCH CENTER, MOFFETT FIELD, CALIFORNIA

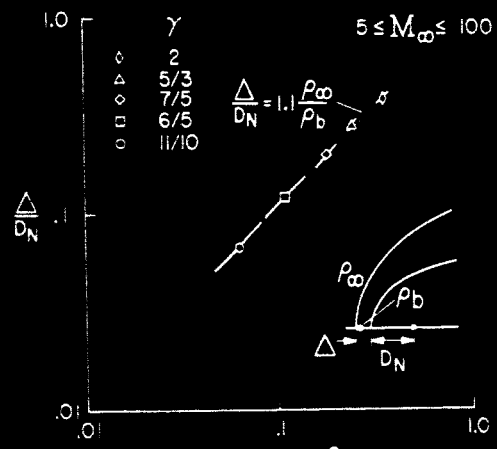

Fig. 6. Variation of standoff distance with density ratio across the nose of the bow shock wave.

NATIONAL AERONAUTICS AND SPACE ADMINISTRATION
AMES RESEARCH CENTER, MOFFETT FIELD, CALIFORNIA